Inorganic Chemistry

Article

pubs.acs.org/IC

Tetranuclear and Pentanuclear Compounds of the Rare-Earth Metals: Synthesis and Magnetism

Munendra Yadav,[†] Abhishake Mondal,[†] Valeriu Mereacre,[†] Salil Kumar Jana,[†] Annie K. Powell,*[,†,‡] and Peter W. Roesky*[,†]

[†]Institut für Anorganische Chemie, Karlsruher Institut für Technologie (KIT), Engesserstrasse 15, 76131 Karlsruhe, Germany

[‡]Institut für Nanotechnologie, Karlsruher Institut für Technologie (KIT), Postfach 3640, D-76021 Karlsruhe, Germany

Supporting Information

ABSTRACT: The Schiff-base proligand 4-*tert*-butyl-2,6-bis-[(2-hydroxyphenylimino)methyl]phenol (H_3L) was prepared in situ from 4-*tert*-butyl-2,6-diformylphenol and 2-aminophenol. The proligand (H_3L) was used with dibenzoylmethane (DBMH) or acetylacetone (acacH) with lanthanides giving compounds with varying arrangements of metal atoms and nuclearities. The tetranuclear compound $\{[Dy_4(L)_3(DBM)_4][Et_3NH]\}$ (**1**) and pentanuclear compound $\{[Dy_5(\mu_3\text{-}OH)_2(L)_3(DBM)_4(MeOH)_4]\cdot 4(MeOH)\}$ (**2**) were obtained from the ligand $(L)^{3-}$ and dibenzoylmethane. The tetranuclear compounds $\{[Dy_4(\mu_4\text{-}OH)(L)_2(acac)_4(MeOH)_2(EtOH)(H_2O)]\cdot(NO_3)\cdot 2(MeOH)\cdot 3(EtOH)\}$ (**3**) and $\{[Ln_4(\mu_3\text{-}OH)_2(L)(HL)(acac)_5(H_2O)]\ (HNEt_3)(NO_3)\cdot 2(Et_2O)\}$ (Ln = Tb (**4**), Dy (**5**), Ho (**6**), and Tm (**7**)) resulted when the ligand $(L)^{3-}$ was used in the presence of acetylacetone. In the solid state structures, the tetranuclear compound **1** adopts a linear arrangement of metal atoms, while tetranuclear compound **3** has a square grid arrangement of metal atoms, and tetranuclear compounds **4**−**7** have a seesaw-shaped arrangement of metal atoms. The composition found from single-crystal X-ray analysis of compound **1** and **3**−**7** is supported by electrospray ionization mass spectrometry (ESI-MS). The magnetic studies on compounds **1** suggest the presence of weak ferromagnetic interactions, whereas compounds **2**−**6** exhibit weak antiferromagnetic interactions between neighboring metal centers. Compounds **1**, **2**, and **3** also show single-molecule magnet behavior under an applied dc field.

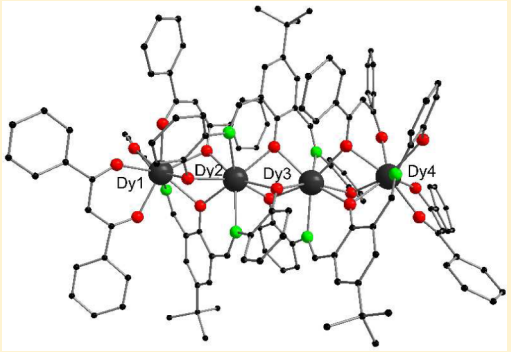

INTRODUCTION

The synthesis of molecular lanthanide compounds has attracted intense research interest due to their applications in catalysis,[1−3] luminescence,[4−8] and magnetism.[9−13] In terms of magnetism, 4f coordination[10] and organometallic[14] compounds have been extensively investigated for their single-molecule magnet (SMM) and single-ion magnet (SIM) properties.[9,11,12,15−23] Potential applications of SMMs are high-density data storage, molecular spintronics, and quantum computing devices.[24−30] The general approach for new SMMs is to aim for systems with large ground spin states and enhanced negative Ising (or easy axis) magnetoanisotropy (D).[22,31−34] Easy axis means that the magnetization is preferentially oriented along one direction. In 4f metal chemistry the coordination compounds of Tb(III), Ho(III), and especially Dy(III) were extensively studied as SMMs in the last few years.[35−59] They feature high spins and intrinsic magnetic anisotropy along with strong spin-orbit coupling. Different structural motifs, e.g., cage complexes,[47,52,56] triangular,[60−64] and linear trinuclear[65,66] and tetranuclear[53,58,67−71] and pentanuclear [72] compounds, have been realized.

Recently, we reported on mono- and polynuclear dysprosium compounds formed using various Schiff-base ligands.[73] For example, by using the multidentate proligand 2,2′-{[(2-aminoethyl)imino]bis[2,1-ethanediyl-nitriloethylidyne]}bis-2-hydroxy-benzoic acid (H_4L') as ligand, the mononuclear Dy(III) complex $[Dy(H_3L')_2](NO_3)\cdot(EtOH)\cdot 8(H_2O)$ showing SIM behavior was obtained.[59] In addition, the ligand 2-aminoethyl-hydroxybenzoic acid (H_2L'') was synthesized and gave the tetranuclear Dy(III) complex $[Dy_4(HL)_2(L)_4(\mu_3\text{-}OH)_2]\cdot 5(MeOH)_2\cdot 7(H_2O)$ showing SMM behavior with two relaxation processes, one with an effective energy barrier U_{eff} = 84 cm^{-1} and pre-exponential factor $\tau_0 = 5.1 \times 10^{-9}$ s.[74]

Now we report an approach in which we combine Schiff-base ligands with either acetylacetone (acac) or dibenzoylmethanide (DBM) as coligands. Both kinds of ligands have been used previously for the synthesis of rare-earth compounds, which were studied in terms of their magnetic properties.[56,75,76] It is known that polynuclear lanthanide clusters can be formed using DBM as ligand or coligand with amino acids or peptoids,[56,77−82] as we, e.g., recently reported with the synthesis of the novel pentadecanuclear lanthanide hydroxyl cluster $[\{Ln_{15}(\mu_3\text{-}OH)_{20}(PepCO_2)_{10}(DBM)_{10}Cl\}Cl_4]$ (Ln = Y, Eu, Tb, Dy; $PepCO_2$ = 2-[{3-(((*tert*-butoxycarbonyl)amino)methyl)-benzyl}amino]acetate).[81,82] Here we report a Schiff-base ligand

Received: April 20, 2015
Published: July 28, 2015

DOI: 10.1021/acs.inorgchem.5b00899
Inorg. Chem. 2015, 54, 7846−7856

combining with DBM or acac as coligands, giving new tetranuclear and pentanuclear lanthanide compounds, which were investigated in terms of their magnetic behavior.

EXPERIMENTAL SECTION

General Considerations. IR spectra were obtained on a Bruker FTIR Tensor 37 via the attenuated total reflection method (ATR). Elemental analyses were carried out with an Elementar vario EL or Vario Micro Cube. Electrospray ionization mass spectrometry (ESI-MS) was performed in positive and negative ionization mode using an *IonSpec* FT-ICR (7T). NMR spectra were recorded on a Bruker Avance II 300 MHz NMR spectrometer. Chemical shifts are referenced to internal solvent resonances and given with respect to tetramethylsilane. All other chemicals were purchased from commercial sources and used without further purification.

Magnetic Measurements. The magnetic measurements were carried out using a Quantum Design MPMS-XL SQUID magnetometer. This magnetometer works between 1.8 and 400 K for dc applied fields ranging from −70 to +70 kOe. Measurements were performed on the polycrystalline samples dispersed in Apiezon grease.

Synthesis of 4-*tert*-Butyl-2,6-bis[(2-hydroxy-phenylimino)-methyl]phenol (H_3L). H_3L was synthesized by condensation of 4-*tert*-butyl-2,6-diformylphenol (82.4 mg 0.4 mmol) and 2-aminophenol (87.3 mg 0.8 mmol) in 15 mL of methanol. The solution was refluxed for 1 h at 80 °C and then cooled to room temperature. A red solid was obtained after evaporating the solvent in vacuum. The solid was further purified by column chromatography (ethyl acetate/pentane 90:10). Yield: 120.4 mg (77.5%). EI-MS: m/z = 388.16. ^{1}H NMR (300 MHz, $CDCl_3$): δ 8.84 (s, 2H, −CH═N—), 7.79 (s, 2H aromatic-H), 7.14 (t, J = 6.6 Hz, 4H, aromatic-H), 7.07 (d, 2H, J = 7.7 Hz, aromatic-H), 6.81 (t, 2H, J = 7.3 Hz, aromatic-H), 1.34 (s, 9H, $-C(CH_3)_3$). $^{13}C\{^1H\}$ NMR (75 MHz): δ 162.89, 157.54, 151.74, 140.82, 134.12, 131.94, 128.85, 120.88, 120.05, 117.93, 116.44, 34.12, 31.26.

*Synthesis of {[Dy_4(L)$_3$(DBM)$_4$]Et_3NH} (**1**).* The Schiff base (H_3L) was prepared in situ by condensation of 4-*tert*-butyl-2,6-diformylphenol (61.8 mg 0.3 mmol) and 2-aminophenol (65.4 mg 0.6 mmol) in 10 mL of acetonitrile (MeCN). The reaction solution was refluxed for 1 h at 80 °C and then cooled to room temperature. $Dy(NO_3)_3{\cdot}5H_2O$ (175.2 mg 0.4 mmol), dibenzoylmethane (100.0 mg 0.4 mmol), and Et_3N (0.15 mL) were subsequently added, and the mixture was refluxed for 1 h. The resulting red solution was filtered, and 0.5 mL of methanol was allowed to diffuse into the solution. It was left undisturbed to allow slow evaporation of the solvent. Yellow single crystals of **1** suitable for X-ray diffraction analysis formed after 3 days.

Yield: 46 mg (4%, based on the crystals). ESI-MS (MeCN): m/z = 2699.26 ($C_{132}H_{107}Dy_4N_6O_{17}^-$ = anion of **1**). Anal. Calcd for $C_{138}H_{125}Dy_4N_7O_{18}$ (corresponds to **1** + H_2O): C, 58.79; H, 4.47; N, 3.48. Found: C, 58.58; H, 4.61; N, 3.17. IR (ATR): ν 3057(w), 2955(w), 1619(m), 1597(m), 1583(m), 1549(m), 1513(m), 1476(s), 1453(w), 1382(w), 1311(w), 1279(m), 1257(w), 1182(m), 1149(w), 1106(w), 1059(m), 1022(w), 963(w), 940(w), 880(w), 844(w), 822(w), 777(w), 737 (m), 721(s), 687(m), 617(w), 606(m), 589(w), 567(w), 512(s) cm^{-1}.

*Synthesis of {[$Dy_5(\mu_3$-OH)$_2$(L)$_3$(DBM)$_4$(MeOH)$_4$]·4(MeOH)} (**2**).* H_3L was synthesized in situ by condensation of 4-*tert*-butyl-2,6-diformylphenol (41.2 mg 0.2 mmol) and 2-aminophenol (43.6 mg 0.4 mmol) in 15 mL of methanol. The solution was refluxed for 1 h at 80 °C and then cooled to room temperature. $Dy(NO_3)_3{\cdot}5(H_2O)$ (153.3 mg 0.35 mmol), dibenzoylmethane (72.0 mg 0.32 mmol), and Et_3N (0.10 mL) were then added, and the solution was refluxed for 3 h, resulting in a red solution with precipitate. The precipitate was filtered off, dissolved in methanol and dichloromethane, and left at room temperature for crystallization. Within 1 week, yellow crystals of **2** were obtained that were suitable for X-ray diffraction analysis. Yield: 42 mg (4% based on single crystals). Anal. Calcd for $C_{140}H_{140}Dy_5N_6O_{27}$: C, 53.36; H, 4.48; N, 2.67. Found: C, 52.88; H, 4.07; N, 3.68. IR (ATR): 3059(w), 2958(w), 2361(w), 1619(w), 1597(s), 1549(m), 1518(s), 1453(m), 1282(s), 1258(w), 1182(w), 1150(w), 1107(w), 1062(s), 1025(m), 1001(w), 962(w), 942(w), 921(w), 880(m), 843(w), 823(s), 776(w), 741(s), 721(w), 688(m), 632(w), 609(m), 589(w), 569(w), 511(s), 474(m), 446(w) cm^{-1}.

*Synthesis of {[$Dy_4(\mu_4$-OH)(L)$_2$(acac)$_4$(MeOH)$_2$(EtOH)(H$_2$O)]·(NO$_3$)·2(MeOH)·3(EtOH)} (**3**).* The Schiff-base proligand (H_3L) was synthesized in situ by condensation of 4-*tert*-butyl-2,6-diformylphenol (41.2 mg 0.2 mmol) and 2-aminophenol (43.6 mg 0.4 mmol) in 10 mL of MeOH. The solution was refluxed for 1 h at 80 °C and then cooled to room temperature. $Dy(NO_3)_3{\cdot}5(H_2O)$ (175.2 mg 0.4 mmol), acetylacetone (0.51 mL 0.5 mmol), and Et_3N (0.1 mL) were subsequently added, and the reaction solution was stirred for 2 min. The resulting red solution was filtered, and then 1 mL of ethanol was added. The solution was left at room temperature for crystallization. After 1 week, yellow-orange crystals were obtained. Yield: 40 mg, (4.5% based on single crystals). ESI-MS (MeCN): m/z = 1930.17 ($[Dy_4(\mu_4\text{-OH})(L)_2(acac)_4(MeOH)(EtOH)(H_2O)]^+$ = cation of **2** − MeOH). Anal. Calcd for $C_{80}H_{113}Dy_4N_5O_{27}$: C, 43.15; H, 5.11; N, 3.15. Found: C, 43.15; H, 4.33; N, 3.41, IR (ATR): 3612(w), 3055(w), 2954(w), 2865(w), 1619(w), 1582(s), 1548(w), 1516(s), 1475(s), 1453(w), 1374(s), 1305(w), 1286(w), 1259(s), 1182(w), 1154(w), 1108(w), 1061(w), 1035(w), 1019(m), 965(w), 950(w), 921(m), 878(m), 845(w), 823(s), 776(m), 748(s), 655(w), 590(m), 570(w), 507(s), 478(m), 448(w) cm^{-1}.

Synthesis of {[$Ln_4(\mu_3$-OH)$_2$(L)(HL)(acac)$_5$(H$_2$O)] (HNEt$_3$)(NO$_3$)·2(Et$_2$O)} (4−7). The Schiff-base proligand (H_3L) was synthesized in situ by condensation of 4-*tert*-butyl-2,6-diformylphenol (41.2 mg 0.2 mmol) and 2-aminophenol (43.6 mg 0.4 mmol) in 10 mL of MeOH. The solution was refluxed for 1 h at 80 °C and then cooled to room temperature. $Ln(NO_3)_3{\cdot}x(H_2O)$ (0.4 mmol) (Ln = Tb, Dy, Ho, Tm), acetylacetone (0.51 mL 0.5 mmol), and Et_3N (0.15 mL) were added, and the solution was refluxed for 2 h. The red solution was evaporated in vacuum, and the obtained solid precipitate was recrystallized from diethyl ether. Within 2 days, red crystals were obtained suitable for X-ray diffraction analysis.

*{[$Tb_4(\mu_3$-OH)$_2$(L)(HL)(acac)$_5$(H$_2$O)](HNEt$_3$)(NO$_3$)·2(Et$_2$O)} (**4**).* Tb-$(NO_3)_3{\cdot}6(H_2O)$ (181.2 mg 0.4 mmol). Yield: 36 mg (4% based on single crystals). ESI-MS(MeCN): m/z = 1951.21 ($[Tb_4(\mu_3\text{-OH})_2(L)$-$(HL)(acac)_5(H_2O)]^+$ = cation of **4**). Anal. Calcd for $C_{79}H_{98}Tb_4N_6O_{22}$ (corresponds to **4** − 2Et_2O): C, 44.77; H, 4.66; N, 3.97. Found: C, 44.16; H, 4.34; N, 3.66. IR (ATR): 2957(br), 1584(m), 1559(w), 1540(w), 1515(s), 1477(m), 1455(w), 1379(s), 1293(w), 1258(s), 1203(w), 1150(w), 1108(w), 1060(w), 1018(m), 953(w), 920(w), 880(w), 821(m), 740(s), 667(w), 654(w), 613(w), 588(m), 571(w), 531(w), 507(w) cm^{-1}.

*{[$Dy_4(\mu_3$-OH)$_2$(L)(HL)(acac)$_5$(H$_2$O)](HNEt$_3$)(NO$_3$)·2(Et$_2$O)} (**5**).* Dy-$(NO_3)_3{\cdot}5(H_2O)$ (174.4 mg 0.4 mmol). Yield: 28 mg (3% based on single crystals). ESI-MS(MeCN): m/z 1966.05 ($[Dy_4(\mu_3\text{-OH})_2(L)$-$(HL)(acac)_5(H_2O)]^+$ = cation of **5**), Anal. Calcd for $C_{79}H_{98}Dy_4N_6O_{22}$ (corresponds to **5** − 2Et_2O): C, 44.47; H, 4.63; N, 3.94. Found: C, 43.90; H, 4.34; N, 3.66. IR (ATR): 2961(br), 1585(m), 1545(w), 1516(s), 1477(m), 1452(w), 1380(s), 1294(w), 1259(s), 1202(w), 1185(w), 1149(w), 1095(w), 1061(w), 1018(s), 962(w), 920(w), 879(w), 820(s), 798(w), 739(s), 686(w), 656(w), 614(w), 588(m), 572(w), 532(w), 507(w) cm^{-1}.

*{[$Ho_4(\mu_3$-OH)$_2$(L)(HL)(acac)$_5$(H$_2$O)](HNEt$_3$)(NO$_3$)·2(Et$_2$O)} (**6**).* Ho-$(NO_3)_3{\cdot}6(H_2O)$ (183.6 mg 0.4 mmol). Yield: 38 mg, (4% based on single crystals). ESI-MS(MeCN): m/z 1974.95 ($[Ho_4(\mu_3\text{-OH})_2(L)$-$(HL)(acac)_5(H_2O)]^+$ = cation of **6**). Anal. Calcd for $C_{87}H_{118}Ho_4N_6O_{22}$ (corresponds to **6**): C, 45.60; H, 5.19; N, 3.67. Found: C, 45.47; H, 5.06; N, 3.18. (ATR): 2958(br), 1585(m), 1559(w), 1540(w), 1517(s), 1477(m), 1456(m), 1437(w), 1419(w), 1383(s), 1295(w), 1258(s), 1236(w), 1185(w), 1152(w), 1108(w), 1061(w), 1018(m), 952(w), 921(w), 880(m), 849(w), 822(s), 740(s), 667(w), 655(w), 614(w), 589(m), 571(w), 532(w), 504(w) cm^{-1}.

*{[$Tm_4(\mu_3$-OH)$_2$(L)(HL)(acac)$_5$(H$_2$O)](HNEt$_3$)(NO$_3$)·2(Et$_2$O)} (**7**).* Tm-$(NO_3)_3{\cdot}5(H_2O)$ (178.0 mg 0.4 mmol). Yield: 46 mg, (5% based on single crystals). ESI-MS (MeCN): m/z 1991.13 ($[Tm_4(\mu_3\text{-OH})_2(L)$-$(HL)(acac)_5(H_2O)]^+$ = cation of **7**). Anal. Calcd for $C_{79}H_{98}Tm_4N_6O_{22}$ (corresponds to **7** −2Et_2O): C, 43.94; H, 4.57; N, 3.89. Found: C, 43.31; H, 4.42; N, 3.56. IR: 2958(br), 1586(m), 1559(w), 1541(w),

DOI: 10.1021/acs.inorgchem.5b00899
Inorg. Chem. 2015, 54, 7846−7856

Table 1. Crystallographic Details of 1−7

	1	2	3	4	5	6	7
chemical formula	$C_{144}H_{144}Dy_4N_8O_{22}$	$C_{140}H_{140}Dy_5N_6O_{27}$	$C_{80}H_{113}Dy_4N_5O_{27}$	$C_{87}H_{118}N_6O_{24}Tb_4$	$C_{87}H_{118}N_6O_{24}Dy_4$	$C_{87}H_{118}N_6O_{24}Ho_4$	$C_{87}H_{118}N_6O_{24}Tm_4$
formula mass	2988.66	3151.13	2226.79	2267.55	2281.87	2291.61	2307.63
cryst syst	triclinic	orthorhombic	orthorhombic	triclinic	triclinic	triclinic	triclinic
a (Å)	12.229(2)	27.378(6)	31.154(6)	13.9775(5)	13.9386(5)	13.9761(5)	13.9186(5)
b (Å)	19.215(4)	29.921(6)	11.549(2)	17.7557(5)	17.7302(5)	17.7491(5)	17.6449 (5)
c (Å)	29.152(6)	32.547(7)	24.197(5)	21.8287(8)	21.7811(8)	21.7385(8)	21.6536(8)
α (deg)	104.58(3)			68.762(2)	68.213(2)	68.770(2)	68.463(2)
β (deg)	96.87(3)			85.665(3)	85.236(3)	85.545(3)	85.537(3)
γ (deg)	95.90(3)			72.449(2)	72.539(2)	72.455(2)	72.381(2)
unit cell volume/Å^3	6519.0(2)	26662(9)	8706(3)	4811.0(3)	4765.6(3)	4789.7(3)	4711.3(3)
temperature/K	150(2)	150(2)	100(2)	150(2)	150(2)	150(2)	150(2)
space group	*P*-1	*Pbca*	$Pna2_1$	*P*-1	*P*-1	*P*-1	*P*-1
no. of formula units per unit cell, Z	2	8	4	2	2	2	2
radiation type	Mo Kα	Mo Kα	Mo Kα	Mo Kα	Mo Kα	Mo Kα	Mo Kα
abs coefficient, μ/mm^{-1}	2.338	2.841	3.472	2.975	3.172	3.339	3.802
no. of reflns measured	61 771	90 588	44 012	31 657	29 926	46 201	101 737
no. of independent reflns	23 782	23 834	14 746	16 371	15 531	16 619	16 606
R_{int}	0.0768	0.0865	0.0843	0.1350	0.0529	0.1522	0.1169
final R_1 values ($I > 2\sigma(I)$)	0.0412	0.0469	0.0555	0.0815	0.0401	0.0783	0.0350
final $wR(F^2)$ values (all data)	0.0811	0.0870	0.1419	0.1652	0.0743	0.1694	0.0903
goodness of fit on F^2	0.891	0.868	0.979	0.902	0.775	0.936	1.022

DOI: 10.1021/acs.inorgchem.5b00899
Inorg. Chem. 2015, 54, 7846−7856

Scheme 1. Synthesis of 1−7

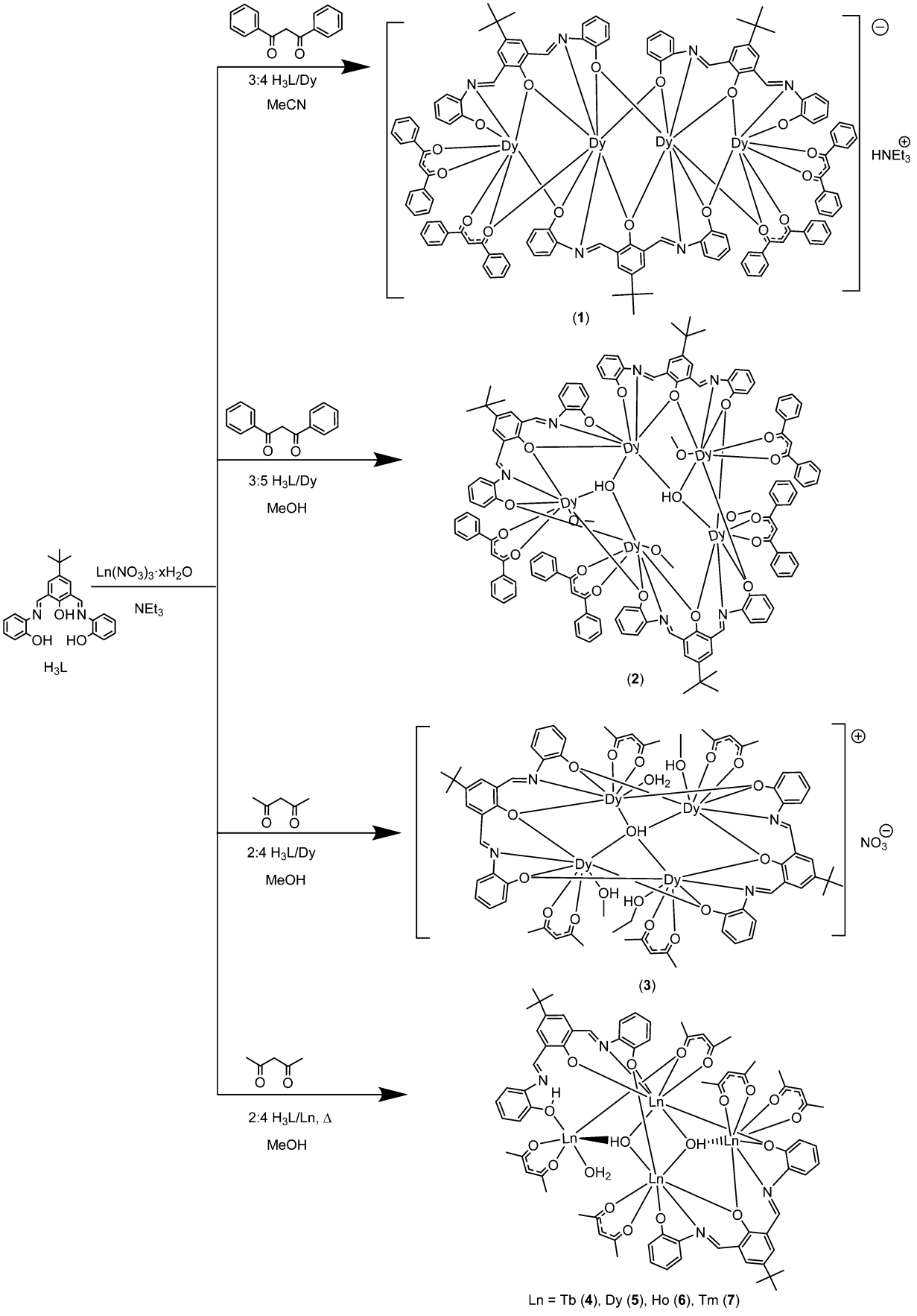

DOI: 10.1021/acs.inorgchem.5b00899
Inorg. Chem. 2015, 54, 7846−7856

1517(s), 1479(m), 1456(w), 1384(s), 1283(w), 1260(m), 1236(w), 1204(w), 1185(w), 1152(w), 1107(w), 1059(w), 1019(m), 961(w), 921(w), 880(w), 849(w), 824(m), 740(s), 688(w), 655(w), 613(w), 590(w), 572(w), 532(w), 506(w) cm^{-1}.

X-ray Crystallographic Studies of 1−7. A suitable crystal was covered in mineral oil (Aldrich) and mounted on a glass fiber. The crystal was transferred directly to a −73 or −123 °C cold stream of a STOE IPDS II diffractometer. All structures were solved using the program SHELXS-97.[83] Further non-hydrogen atoms were located from successive Fourier difference map calculations. The refinements were carried out using the full-matrix least-squares techniques on F^2, minimizing the function $(F_0 - F_c)^2$, where the weight is defined as $4F_0^2/2(F_0^2)$ and F_0 and F_c are the observed and calculated structure factor amplitudes using the program SHELXL-97.[83] The hydrogen atoms were placed in their calculated positions without refinement. The final values of refinement parameters are given in Table 1. The locations of the largest peaks in the final difference Fourier map calculation as well as the magnitude of the residual electron densities in all cases were of no chemical significance. Positional parameters, thermal parameters, bond distances, and angles have been deposited as Supporting Information.

RESULTS AND DISCUSSION

Synthesis and Structures. We report here on multinuclear rare-earth complexes ligated by 4-*tert*-butyl-2,6-bis[(2-oxyphenylimino)-methyl]-phenolate (L^{3-}). We synthesized the Schiff-base proligand H_3L by refluxing 4-*tert*-butyl-2,6-diformylphenol and 2-aminophenol in methanol and characterized it. During our investigation, we realized that in situ preparation without isolation of H_3L is most efficient. The in situ prepared proligand H_3L was refluxed with $[Dy(NO_3)_3{\cdot}5(H_2O)]$ and the appropriate coligand (acetylacetone or dibenzoylmethane) to obtain the tetranuclear and pentanuclear compounds as single-crystalline material. Triethylamine was used as a base to deprotonate the proligand (H_3L), and coligand dibenzoylmethane, or acetylacetone. The stoichiometric ratio of metal to ligand, solvents, coligand, and the reaction conditions played a key role in the formation of these compounds. The proligand (H_3L) was stirred with dibenzoylmethane in the stoichiometric ratio of 3:4:4 (H_3L:Ln:DBMH) in acetonitrile to get the tetranuclear compound $\{[Dy_4(L)_3(DBM)_4][Et_3NH]\}$ (**1**) (Scheme 1). The pentanuclear compound $\{[Dy_5(\mu_3\text{-}OH)_2(L)_3(DBM)_4(MeOH)_4]{\cdot}4(MeOH)\}$ (**2**) was obtained by altering the solvent to methanol and the stoichiometry ratio to 2:3.5:3.2 (H_3L:Ln:DBMH). Compound **2** was separated as a powder by filtration from the reaction mixture; then it was recrystallized from methanol and dichloromethane to obtain the single-crystalline material. When the coligand DBM was replaced by acetylacetone and the stoichiometric ratio by 2:4:5 (H_3L:Ln:acacH), the tetranuclear compounds $\{[Dy_4(\mu_4\text{-}OH)(L)_2(acac)_4(MeOH)_2(EtOH)(H_2O)]{\cdot}(NO_3){\cdot}2(MeOH){\cdot}3(EtOH)\}$ (**3**) and $\{[Dy_4(\mu_3\text{-}OH)_2(L)(HL)(acac)_5(H_2O)]\ (HNEt_3)(NO_3){\cdot}2(Et_2O)\}$ (**5**) were obtained. For the latter compound also the analogue complexes $\{[Ln_4(\mu_3\text{-}OH)_2(L)(HL)(acac)_5(H_2O)]\ (HNEt_3)(NO_3){\cdot}2(Et_2O)\}$ (Ln = Tb (**4**), Ho (**6**), and Tm (**7**)) were synthesized starting from the corresponding nitrates $[Ln(NO_3)_3{\cdot}x(H_2O)]$ (Ln = Tb, Ho, and Tm). Compound **3** was isolated directly from the reaction mixture when the proligand (H_3L) was stirred with dysprosium nitrate and acetylacetone for 2 min at room temperature. Further, by altering the reaction time by 2 h, compound **5** was isolated as single-crystalline material by recrystallization of the reaction mixtures in diethyl ether. Compounds **4** and **5**−**7** were prepared in an analogous way. The solid state structures of **1**−**7** were established by single-crystal-X-ray diffraction. Furthermore, all compounds were characterized by spectroscopic and analytical techniques. Compounds **1** and **3**−**7** were additionally characterized by ESI-MS, whereas for **2** no suitable ESI-MS could be acquired. Since we were interested in the magnetic properties of our newly synthesized compounds, we used only single-crystalline material for further investigations. For all compounds we thus determined the yields only based on the single-crystalline material. This results in relatively low yields of the very pure material.

The centrosymmetric complex $\{[Dy_4(L)_3(DBM)_4][Et_3NH]\}$ (**1**) crystallized in the triclinic space group *P*-1 with two molecules in the unit cell. Compound **1** consists of a $[Dy_4(DBM)_4(L)_3]^-$ anion and a protonated triethylamine countercation. The anion consists of four Dy(III) ions coordinated by three central trianionic Schiff-base ligands $(L)^{3-}$ and four peripheral monoanionic DBM ligands. The molecular structure of the anion $[Dy_4(DBM)_4(L)_3]^-$ is shown in Figure 1. The dysprosium atoms in compound **1** are 8-fold

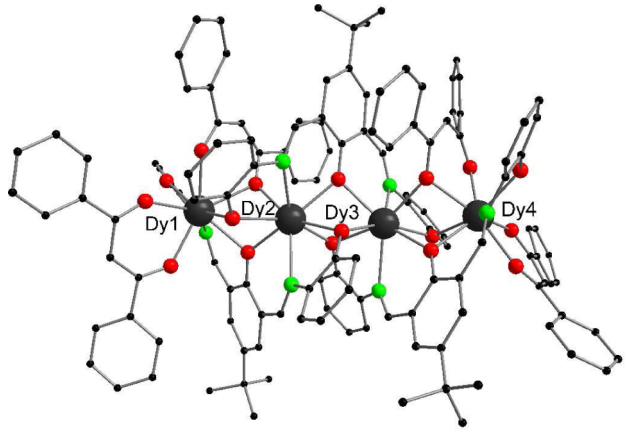

Figure 1. Solid state structure of the cation of **1**; shown is the coordination arrangement of a dysprosium, omitting hydrogen atoms for clarity. Color code of balls: Dy, dark gray; O, red; N, green; C, black.

coordinate and feature a distorted square antiprism coordination geometry. Each central Dy atom (Dy2 and Dy3) is coordinated by two nitrogen atoms and five oxygen atoms (μ_2-bridging modes) of the Schiff-base ligands and one μ_2-bridging oxygen atom of the DBM ligand. Each peripheral Dy atom (Dy1 and Dy4) is coordinated to one nitrogen atom and seven oxygen atoms; two oxygen atoms of the Schiff-base ligands and one oxygen atom of the DBM ligand show the μ_2-bridging coordination modes. The Dy_4 metal core of complex **1** is essentially linear as evidenced by angles of Dy3−Dy2−Dy1 163.798(12)° and Dy2−Dy3−Dy4 165.562(12)°. These angles are in line with those of the previously reported tetranuclear dysprosium complexes $[Dy_4(L)_4(MeOH)_6]$[58] (H_3L = 2-hydroxy-3-methoxybenzoic acid [(2-hydroxy-3-methoxyphenyl)methylene] hydrazide) and $[Dy_4(L)_2(C_6H_5COO)_{12}(CH_3OH)_4]$[67] (HL = 2,6-bis((furan-2-ylmethylimino)methyl)-4-methylphenol), which have Dy−Dy−Dy angles of 149.99° and 175.673°, respectively. The distances between the Dy(III) metal ions in **1** are Dy1−Dy2 3.5126(9) Å, Dy2−Dy3 3.4497(9) Å, and Dy3−Dy4 3.4805(8) Å, which are slightly shorter than previously reported linear tetranuclear compounds.[58,67,68] The reported linear tetranuclear compound $[Dy_4(L)_4(HL)_2(C_6H_4NH_2COO)_2(CH_3OH)_4]$ (H_2L = *N*-(2-

DOI: 10.1021/acs.inorgchem.5b00899
Inorg. Chem. 2015, 54, 7846−7856

carboxyphenyl)salicylidenimine) has Dy−Dy distances between 4.055 and 4.241 Å.[68] The bond distances of Dy−O and Dy−N are in the range 2.259(4)−2.411(4) and 2.486(5)−2.542(5) Å respectively, which are comparable to reported complexes.[32,33]

Compound $\{[Dy_5(\mu_3\text{-}OH)_2(L)_3(DBM)_4(MeOH)_4]\cdot 4(MeOH)\}$ (**2**) crystallizes in the orthorhombic space group *Pbca* with eight molecules in the unit cell. The metal ions are encapsulated by four monoanionic dibenzoylmethanide ligands, three trianionic ligands $(L)^{3-}$, and two hydroxyl ions. A view of complex **2** is shown in Figure 2. The pentanuclear complex has

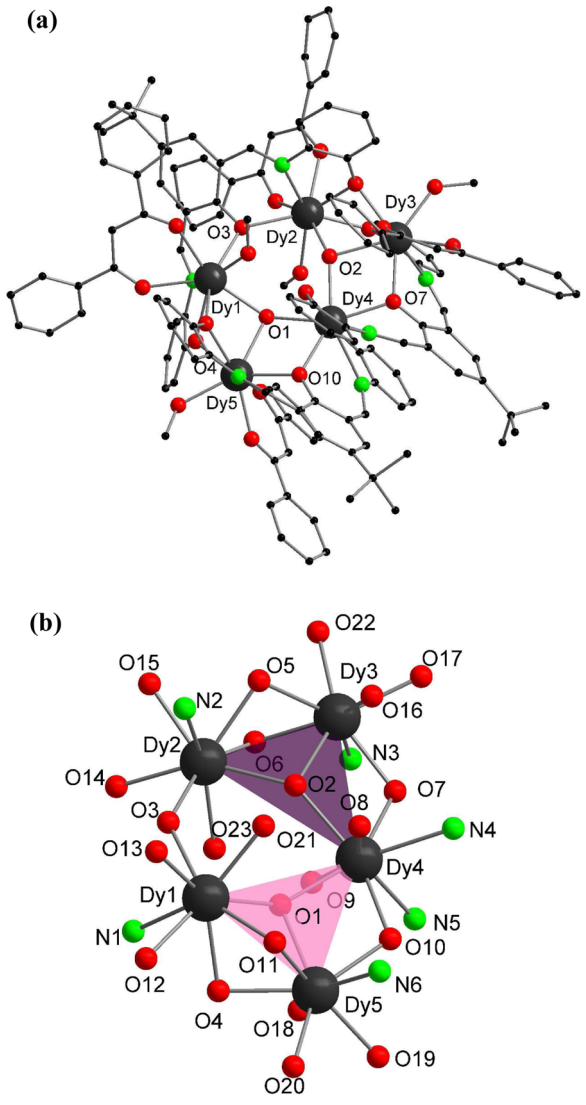

Figure 2. (a) Solid state structure of **2**, and (b) side view of the Dy_5 metal core. All hydrogen atoms and solvent molecules have been omitted for clarity.

an interesting topology. In contrast to the **2** examples of Dy_5 reported in the literature, which have a square-based pyramidal or trigonal bipyramidal arrangement of the metal centers (but with different connections between the metal centers), the metal atoms of the central core $[Dy_5(\mu_3\text{-}OH)_2(\mu_2\text{-}O)_7]$ are in an almost coplanar arrangement as a " bow-tie" motif.[39,52,56,84] The core motif can be described in terms of two triangles of Dy A (Dy1, Dy4, Dy5) and B (Dy2, Dy3, Dy4); sharing a common vertex (Dy4), with μ_3-(OH) groups occupying the center of these triangles. The triangles A and B are shown in the metal core by rose and plum color, respectively (see Figure 2b). The essentially identical triangles A and B sharing Dy4 as common vertex are also bridged by O3. The μ_3-(OH) groups (O1, O2) nearly symmetrically bridge the metal centers and lie 0.524 Å below and 0.532 Å above the plane of the metal cores, respectively. The Dy−(μ_3-O1) bond lengths are in range of 2.363(5)−2.415(5) Å, and those are comparable with the Dy−(μ_3-O2) bond lengths of 2.374(5)−2.423(5) Å. The atom (O3) is nearly symmetrically bound to both triangles A and B with regard to bond lengths Dy1−O3 2.408(5) Å and Dy2−O3 2.425(6) Å. The phenolate oxygen atoms of the Schiff bases are in μ_2-bridging modes, except O8 and O9 which are in η^1-modes. All O atoms of the DBM ligand are in κ^2-modes. Each Dy(III) ion of the complex is 8-fold coordinate, and the coordination geometry is best described as distorted square antiprismatic. Dy1, Dy2, Dy3, and Dy5 are coordinated to two O atoms of the DBM ligand, one O atom from hydroxide, one molecule of methanol, three O atoms, and one N atom of the Schiff-base ligands. The Dy4 coordination sphere ($N2O6$) consists of six O atoms and two N atoms of the Schiff-base ligands. The Dy−O and Dy−N bond distances are in the range 2.289(5)−2.425(6) and 2.487(6)−2.563(6) Å, respectively. The Dy−Dy distances are in the range of 3.5282(7)−3.7983(9) Å, which are comparable to the reported $[Dy_5(\mu_3\text{-}OH)_6(Acc)_6(H_2O)_{10}]^{9+}$ (Acc = 1-amino-cyclohexanel-carboxylic acid) Dy−Dy distances of 3.7100(5)−3.8721(4).[84]

Compound $\{[Dy_4(\mu_4\text{-}OH)(L)_2(acac)_4(MeOH)_2(EtOH)(H_2O)]\cdot(NO_3)\cdot 2(MeOH)\cdot 3(EtOH)\}$ (**3**) crystallizes in the orthorhombic space group $Pna2_1$ with four molecules in the unit cell. The asymmetric unit consists of a $[Dy_4(\mu_4\text{-}OH)(L)_2(acac)_4(MeOH)_2(EtOH)(H_2O)]^+$ cation and a nitrate counteranion. The molecular structure of the cation is shown in Figure 3. The charge of the four Dy(III) ions in the complex ion is balanced by four monoanionic acac ligands, two trianionic Schiff-base ligands $(L)^{3-}$, one hydroxide ion, and the nitrate counteranion. The central metal core of complex **3** consists of four Dy(III) ions, which are arranged in a square grid shape around the central μ_4-(OH) ion. This 4-fold metal bridging mode causes the folding of the Dy4-square. The four Dy(III) ions are thus not localized in a plane but rather adopt a butterfly structure. Square grid arrangements are relatively rare in the literature, e.g., in $\{[Dy_4(\mu_4\text{-}OH)(Hhpch)_8)]\cdot(ClO_4)_3\}$ (H_2hpch = 2-hydroxylbenzaldehyde (pyridine-4-carbonyl) hydrazone)[55] and $[Dy_4(L1{-}2H)_2(L1\text{-}H)_2(N_3)_4(O)]$.[21]

In compound **3**, each Schiff-base coordinates to all four Dy(III) ions with μ_2-bridging phenolate oxygen atoms (O2, O3, O4, O5, O6, and O7) and imine nitrogen atoms (N1, N2, N3, and N4). Each Dy(III) ion binds to the central μ_4-(OH) ion. The central group is assigned as an OH group as a result of the charge balance. Note it is not possible to unambiguously assign the position of the remaining proton. The 8-fold coordination sphere of each Dy(III) ion is completed by the $(L)^{3-}$ ligands, one acac ligand, and one methanol (Dy1 and Dy3) or ethanol (Dy4) or water molecule (Dy2). Each Dy(III) ion is coordinated by seven oxygen atoms and one imine nitrogen atom and features a distorted square antiprism coordination geometry. The Dy−(μ_2-O) bond distances (2.288(11)−2.333(11) Å) are slightly shorter than the Dy−(μ_4-OH) bond distances (2.473(11)−2.636(11) Å). The arrangement of the Dy(III) ions and μ_2-bridged phenolate oxygen atoms adopts an octagonal shape, which is shown in the metal core of the compound (see Figure 3). The Dy−N bond lengths range from 2.503(14) to 2.536(15) Å, and the Dy−Dy

DOI: 10.1021/acs.inorgchem.5b00899
Inorg. Chem. 2015, 54, 7846−7856

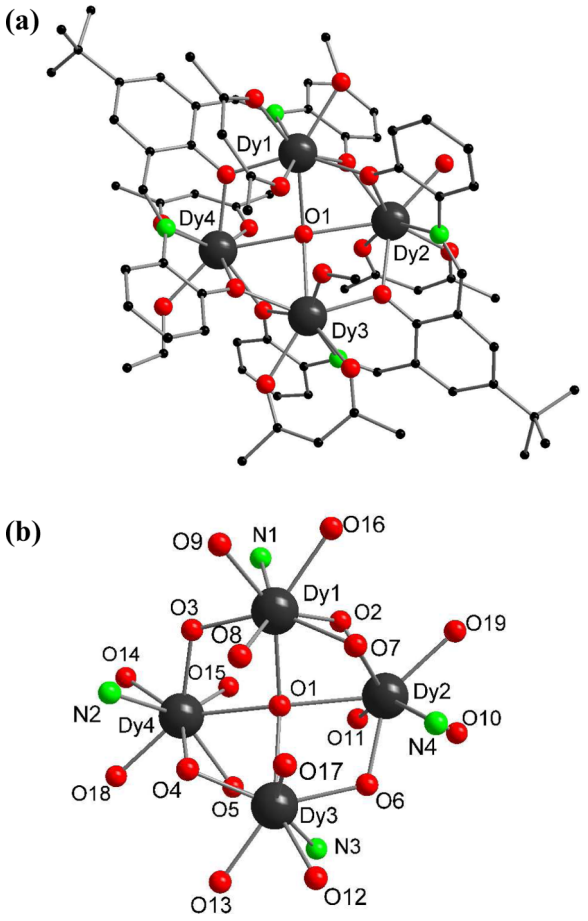

Figure 3. (a) Solid state structure of the cation of **3**, and (b) side view of the square grid Dy_4 metal core. All hydrogen atoms and solvent molecules have been omitted for clarity.

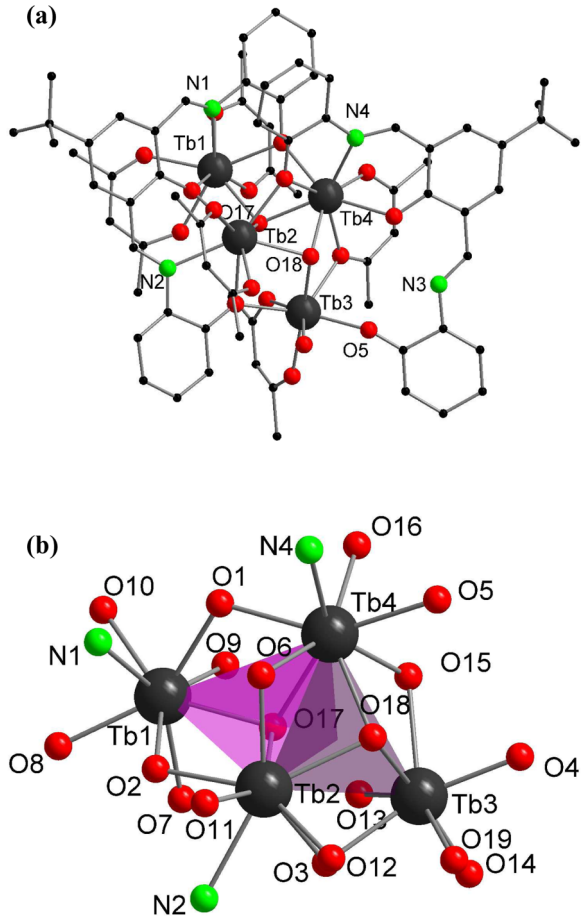

Figure 4. (a) Solid state structure of the cation of **4**, and (b) side view of the seesaw shaped Tb_4 metal core. All hydrogen atoms and solvent molecules have been omitted for clarity.

distances range from 3.5346(12) to 3.8994(13) Å. The bond distances of compound **3** are in a comparable range to the reported tetranuclear square grid complex $[Dy_4(L1\text{-}2H)_2(L1\text{-}H)_2(N_3)_4(O)]$ (L1 = a ditopic carbohydrazone ligand), which have Dy−N bond lengths of 2.34−2.56 Å and Dy−Dy distances of 3.66−3.69 Å.[21]

Complexes $\{[Ln_4(\mu_3\text{-}OH)_2(L)(HL)(acac)_5(H_2O)](HNEt_3)(NO_3)\cdot 2(Et_2O)\}$ (Ln = Tb (**4**), Dy (**5**), Ho (**6**), and Tm (**7**)) crystallize in the triclinic space group *P*-1 with two molecules in the unit cell and form an isostructural series. Thus, only the representative bonding parameters of **4** are discussed in detail (Figure 4). The asymmetric unit of compounds **4**−**7** consists of one $[Ln_4(\mu_3\text{-}OH)_2(L)(HL)(acac)_5(H_2O)]$ molecule. Furthermore, one triethylamonium nitrate ion pair and two diethyl ether molecules are present in the crystal lattice. The charge of the four Dy(III) ions is balanced by one trianionic Schiff base $(L)^{3-}$, one dianionic Schiff base $(HL)^{2-}$, five monoanionic acac ligands, and two hydroxide ions. The composition of compounds (**4**−**7**) is supported by ESI-MS data. Although in the single-crystal X-ray structures some electron density is located between the phenol oxygen atom and the Schiff-base nitrogen atom for $(HL)^{2-}$ (see Scheme 1), it is not possible to unambiguously assign the position of the remaining acidic proton. Since one nitrogen atom (N3) of the dianionic Schiff-base $(HL)^{2-}$ ligand does not coordinate to the metal atom, it is likely the proton is localized between N3 and O5. The metal core consists of a tetranuclear arrangement of Ln(III) ions in a seesaw shape. Such a seesaw-shaped geometry for tetranuclear rare-earth metals $[Ln_4(L)_4(\mu_4\text{-}OH)(\mu_3\text{-}OH)_2(NO_3)_4]\cdot(NO_3)$ (LH = 2-methoxy-6-(pyridin-2-ylhydrazonomethyl)phenol) is rarely reported in the literature.[85] The seesaw shape is made up by two edge-sharing triangles A (Tb1−Tb2−Tb4) and B (Tb2−Tb4−Tb3). Triangles A and B are shown in the metal core as pink- and plum-colored spheres, respectively (see Figure 4). In triangle A, the μ_3-hydroxo group (O17) is located 0.960 Å below the plane of the triangle. In triangle B, the μ_3-hydroxo group (O18) is located 1.047 Å above the plane of the triangle. These triangular planes are oriented at an angle of 71.23° from each other. The angles between the Tb(III) ions are 56.18(2)° (Tb2−Tb3−Tb4) and 54.12(2)° (Tb2−Tb1−Tb4). Tb1, Tb2, and Tb4 are 8-fold coordinate via seven oxygen atoms and one nitrogen atom. Tb1 has a distorted square-antiprismatic coordinate ion sphere of four O atoms of the acac ligands, one μ_3-hydorxyl ions (O17), two μ_2-bridged phenolate oxygen atoms, and one N atom of a Schiff base. Tb2 and Tb4 have distorted square-antiprismatic coordinate ion spheres made up of two μ_3-bridged hydroxyl ions, two oxygen atoms from the acac ligand, and three oxygen atoms and one nitrogen atom of the Schiff-base ligand. Tb3 is coordinated to seven oxygen atoms, and its coordination geometry can be best described as a distorted monocapped octahedron. The Tb−O and Tb−N distances are in the range 2.189(14)−2.496(10) and

DOI: 10.1021/acs.inorgchem.5b00899
Inorg. Chem. 2015, 54, 7846−7856

2.507(14)−2.540(14) Å, respectively. The Tb−Tb distances are in the range 3.5142(11)−3.8752(12) Å.

Magnetic Properties of Compounds 1−6. As some of the linear tetranuclear dysprosium clusters[58,67,68] show SMM behavior, we were interested in studying the magnetic properties of compounds **1**. The dc magnetic susceptibility data for compound **1** was collected in the 1.8−300 K temperature range under a field of 1000 Oe (Figure 5). At

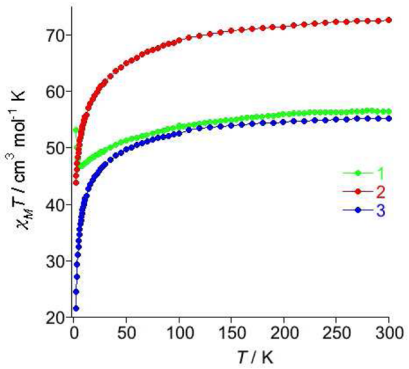

Figure 5. Plots of $\chi_M T$ vs T for compounds **1**, **2** and **3** under 1000 Oe dc field.

300 K, the $\chi_M T$ product of **1** is 56.5 cm^3 mol^{-1} K (Figure 5), in good agreement with the expected value of 56.7 cm^3 mol^{-1} K for four noncoupled Dy(III) metal ions (S = 5/2, L = 5, g = 4/3). Upon cooling, the $\chi_M T$ product decreases smoothly to a value of 46.7 cm^3 mol^{-1} K at 7 K. Then the $\chi_M T$ product increases to a maximum value of 53.2 cm^3 mol^{-1} K at 1.8 K. This low-temperature increase suggests the presence of very weak ferromagnetic exchange between the constituent Dy(III) ions.[62] Magnetization (M) data were collected over the 0−70 kOe field range at different temperatures. The nonsuperposition of the M vs H/T data (Figure S2, Supporting Information) suggests the presence of a significant magnetic anisotropy and/or low-lying excited states. The magnetization increases rapidly at low field to reach a value of 23.5 μ_B at 70 kOe (Figure S1, Supporting Information) without clear saturation. This value is much lower than the expected saturation value of ∼40 μ_B for four noninteracting Dy(III) ions, most likely due to the crystal-field effect at the Dy(III) ion that eliminates the 16-fold degeneracy of the $^6H_{15/2}$ ground state.

Due to the presence of magnetic anisotropy, the magnetization relaxation of this system was probed under zero dc field using ac susceptibility measurements as a function of the temperature at different frequencies. This compound exhibits a broad and weak nonzero out-of-phase ac susceptibility signal (Figure S3, Supporting Information), indicating the absence of any appreciable barrier to relaxation of the magnetization, which could be due to strong quantum tunneling resonance at zero dc field. A clear maximum of the out-of-phase signal could not be observed above 1.8 K at a frequency of 1500 Hz. One of the reasons could be the presence of several relaxation processes with very close energy barriers and blocking temperatures. This hypothesis might be ascertained at a low-temperature regime at Cole−Cole plots (Figure S5, Supporting Information). Such a behavior is expected taking into consideration the presence of several Dy centers. Nevertheless, the weakly frequency-dependent out-of-phase ac susceptibilities signals indicate that this compound exhibits slow magnetic relaxation, probably being a SMM.

In order to further investigate the dynamic magnetic properties of this complex, ac susceptibility measurements in the presence of a weak dc field were performed. The out-of phase and in-phase ac susceptibilities have similar intensity even with the application of an external dc field (Figure S3, Supporting Information). This type of behavior suggests that the slow relaxation is not dominated by quantum tunneling but is the intrinsic property of the molecule with several magnetic centers. Although this compound shows classical SMM-like behavior with strong frequency dependence, the hysteresis of the magnetization is not observable at 2 K (Figure S1, Supporting Information).

As for compound **1**, the dc magnetic data for complex **2** shows a temperature-dependent value of $\chi_M T$ of from 72.74 to 65.12 cm^3 K mol^{-1} over the temperature range 300−50 K (Figure 5). On lowering the temperature, $\chi_M T$ drops abruptly to a minimum value of 43.76 cm^3 K mol^{-1} at 2 K, indicating depopulation of excited Stark sublevels.

The magnetization for complex **2** at different temperatures (2−5 K) reaches a maximum value of 28.38 μ_B at 70 kOe without showing true saturation (Figure S6, Supporting Information). This is noticeably lower than the theoretical value for five Dy(III) ions (∼50 μ_B), indicating a much smaller effective spin and also significant magnetic anisotropy in **2**.

Due to the presence of magnetic anisotropy, the magnetization relaxation of this system has also been probed under zero and nonzero dc fields using ac susceptibility measurements as a function of the temperature at different frequencies. Clearly this compound exhibits nonzero out-of-phase ac susceptibility with a weak intensity (Figure S7, Supporting Information) even in an applied dc field. The frequency-dependent out-of-phase ac susceptibility signals indicate that this compound exhibits slow magnetic relaxation typical for a SMM but with a blocking temperature well below 1.8 K.

At room temperature, the $\chi_M T$ product for compound **3** is 55.1 cm^3 K mol^{-1} (Figure 5). This value is slightly lower than the expected value of 56.6 cm^3 K mol^{-1} for four Dy^{III} (S = 5/2, L = 5, $^6H_{15/2}$) noninteracting ions. On decreasing the temperature, $\chi_M T$ first decreases gradually to 48.4 cm^3 K mol^{-1} at 50 K and then drops more steeply to a value of 21.3 cm^3 K mol^{-1} at 1.8 K. Such behavior is due to thermal depopulation of the Dy^{III} excited states and contribution from the effects of anisotropy. This is in agreement with the magnetization measurements (Figure S9, Supporting Information) which show an increase of magnetization at low temperature but without saturation even at an applied field of 70 kOe. As for the other compounds studied in this work, the magnetization values are in good accord with the susceptibility data and show expected values for four Dy^{III} ions, ∼ 20 μ_B.

The ac susceptibility data in a zero dc field have shown evidence of a slow relaxation of magnetization for **3**. Below 10 K, both χ' and χ'' become frequency dependent. An unusual feature of these curves is that they show two or more peaks that are frequency and temperature dependent (Figure 6) with the maximum for the most clear peak for χ'' at 6.5 K for 1500 Hz, revealing the occurrence of several relaxation processes. Such a behavior has been described in recent several reports[43,86,87] and has been attributed to the occurrence of different Ln^{III} sites in the crystal lattice. This can also be applied to **3**, which has four Dy^{III} centers with different coordination spheres and geometries. It is possible that the slight differences in the local coordination spheres are responsible for the multiple processes. Since the coupling between the Dy^{III} centers is very weak, they

DOI: 10.1021/acs.inorgchem.5b00899
Inorg. Chem. 2015, 54, 7846−7856

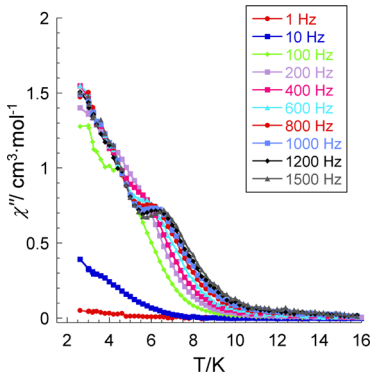

Figure 6. Plots of χ'' vs T with different frequencies under zero dc field for compound **3**.

can behave individually with their own blocking temperature of the magnetization. Therefore, the peaks of the χ' and χ'' signals can be associated with several relaxation times corresponding to each of the four types of Dy^{III} ions in **3**. The assumption of the operation of more than one relaxation process in this compound is also confirmed by Cole−Cole plots (Figure 7).

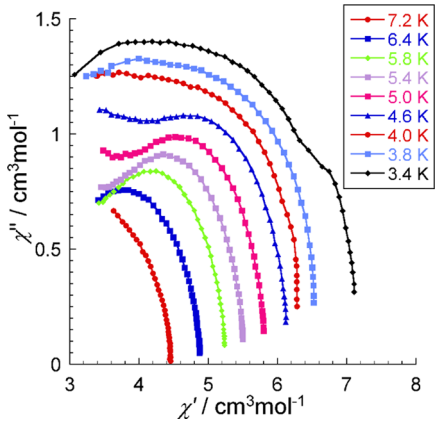

Figure 7. Cole−Cole plots at zero static field from 3.4 to 7.2 K for **3**. Solid lines are guides for eyes.

Because of the strong overlap of peaks at low temperatures, the evaluation of the effective energy barriers for magnetization reversal and relaxation times has been possible only for the high-temperature feature. The data have been analyzed using an Arrhenius law and give an estimate for the energy barrier, Δ/k_B, as 51.5 K with a pre-exponential relaxation time, τ_0, of 3.0×10^{-8} s (Figure S11, Supporting Information). The obtained values are in agreement with the SMM behavior for **3**. An additional indication of a broad distribution of relaxation times at low temperatures, suggesting that more than one relaxation process is in operation, could also be concluded from the frequency-dependent ac susceptibility measurements from 1.8 to 7.2 K (Figure S10, Supporting Information).

The temperature-dependent dc magnetic susceptibility data for compounds **4**, **5**, and **6** were collected in the range 300−1.8 K and in an applied magnetic field of 1000 Oe. The magnetization (M) data were collected in the 0−70 kOe field range at different temperatures (2−5 K).

At room temperature, the χT values of complexes **4**, **5**, and **6** are 44.0, 54.4, and 55.0 cm^3 K mol^{-1}, respectively (Figure 8). These values are in good agreement with the expected

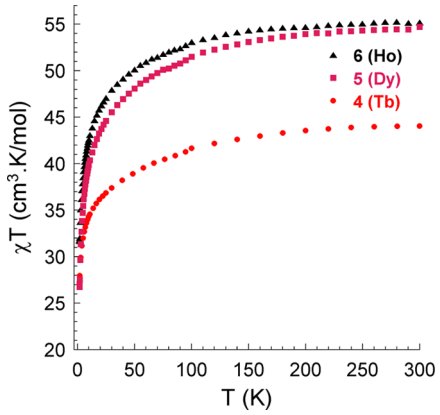

Figure 8. Plots of $\chi_M T$ vs T for compounds **4**, **5**, and **6** under 1000 Oe dc field.

theoretical values (**3**, 47.2 cm^3 K mol^{-1}; **4**, 56.7 cm^3 K mol^{-1}; **5**, 56.3 cm^3 K mol^{-1}) for four noninteracting lanthanide ions: Tb^{III} ($^7F_6$, $S = 3$, $L = 3$, $g = 3/2$, $\chi = 11.82$ cm^3 K mol^{-1}), Dy^{III} ($^6H_{15/2}$, $S = 5/2$, $L = 5$, $g = 4/3$, $\chi = 14.17$ cm^3 K mol^{-1}), and Ho^{III} ($^5I_8$, $S = 2$, $L = 6$, $g = 5/4$, $\chi = 14.08$ cm^3 K mol^{-1}). On lowering the temperature, χT for **4**−**6** remains almost constant until ∼100 K and then decreases sharply to reach a value of 27.0, 27.8, and 31.3 cm^3 K mol^{-1}at 1.8 K for compounds **4**, **5**, and **6**, respectively (Figure 8). For the lanthanide ions, such as Tb^{III}, Dy^{III}, and Ho^{III}, with an unquenched orbital moment associated with a ligand field, the decrease of χT can originate from three main contributions: weak intramolecular antiferromagnetic interactions, thermal depopulation of the Ln^{III} substates, and magnetic anisotropy.

The field dependence of the magnetization for **4**−**6** (Figure S12, Supporting Information) at low temperatures (2, 3, and 5 K) shows that the magnetization increases rapidly at low field and finally reaches values of 18.2, 19.9, and 21.4 μ_B at 70 kOe without clear saturation. These values are much lower than the expected saturation values of four noninteracting Tb^{III}, Dy^{III}, and Ho^{III} ions. The lack of saturation points to the presence of magnetic anisotropy and/or the lack of a well-defined ground state. The low values of saturation are expected for Tb^{III}, Dy^{III}, and Ho^{III} single ions in polycrystalline samples.

The ac susceptibility for **4**−**6** in zero and nonzero (500−3000 Oe) dc field was measured but did not show any sign of slow relaxation of the magnetization within the accessible frequency range. The results for compounds **4**−**6** suggest the absence of slow relaxation of magnetization in compound **7**. Hence, it has not been magnetically studied.

SUMMARY

Novel compounds of rare-earth metals **1** and **2** are ligated with the L^{3-} and dibenzoylmethanide, whereas compounds **3**−**7** are ligated with the L^{3-} and acetylacetone, which were prepared and structurally characterized. The solid state structures of the compounds were established with single-crystal X-ray diffraction. The tetranuclear compounds (**1**, **3**−**7**) and pentanuclear compound (**2**) adopt the different arrangements of the metal ions. Compound **1** shows the weak ferromagnetic interactions, whereas compounds **2**−**6** exhibit weak antiferromagnetic interactions between neighboring metal ions. In addition, compounds **1**, **2**, and **3** show SMM behavior under zero and external dc fields. To the best of our knowledge, **1** is the first

DOI: 10.1021/acs.inorgchem.5b00899
Inorg. Chem. 2015, 54, 7846−7856

linear tetranuclear Dy complex which exhibits weak ferromagnetic interaction between neighboring metal atoms.

■ ASSOCIATED CONTENT

Supporting Information

X-ray crystallographic files in CIF format for the structure determinations of **1**−**7**, and additional information about the magnetic measurements. The Supporting Information is available free of charge on the ACS Publications website at DOI: 10.1021/acs.inorgchem.5b00899.

■ AUTHOR INFORMATION

Corresponding Authors

*E-mail: annie.powell@kit.edu.
*E-mail: roesky@kit.edu.

Notes

The authors declare no competing financial interest.

■ ACKNOWLEDGMENTS

This work was supported by the DFG-funded transregional collaborative research center SFB/TRR 88 "3MET".

■ REFERENCES

(1) Anwander, R. *Lanthanides: Chemistry and Use in Organic Synthesis*; Springer: Berlin, Heidelberg, 1999.
(2) Shibasaki, M.; Yamada, K.-I.; Yoshikawa, N. Lanthanide Lewis Acids Catalysis. In *Lewis Acids in Organic Synthesis*; Wiley-VCH Verlag GmbH: Weinheim, 2008; pp 911−944.
(3) Roesky, P. W. *Molecular Catalysis of Rare-Earth Elements*; Springer: Berlin, Heidelberg, 2010.
(4) Eliseeva, S. V.; Bunzli, J.-C. G. *Chem. Soc. Rev.* **2010**, *39*, 189−227.
(5) Heffern, M. C.; Matosziuk, L. M.; Meade, T. J. *Chem. Rev.* **2014**, *114*, 4496−4539.
(6) Bünzli, J.-C.; Eliseeva, S. Basics of Lanthanide Photophysics. In *Lanthanide Luminescence*; Hänninen, P., Härmä, H., Eds.; Springer: Berlin, Heidelberg, 2011; Vol. 7, pp 1−45.
(7) Mathis, G.; Bazin, H. Stable Luminescent Chelates and Macrocyclic Compounds. In *Lanthanide Luminescence*; Hänninen, P., Härmä, H., Eds.; Springer: Berlin, Heidelberg, 2011; Vol. 7, pp 47−88.
(8) Faulkner, S.; Sykes, D. Lanthanide Assemblies and Polymetallic Complexes. In *Lanthanide Luminescence*; Hänninen, P., Härmä, H., Eds.; Springer: Berlin, Heidelberg, 2011; Vol. 7, pp 161−182.
(9) Sorace, L.; Benelli, C.; Gatteschi, D. *Chem. Soc. Rev.* **2011**, *40*, 3092−3104.
(10) Woodruff, D. N.; Winpenny, R. E. P.; Layfield, R. A. *Chem. Rev.* **2013**, *113*, 5110−5148.
(11) Feltham, H. L. C.; Brooker, S. *Coord. Chem. Rev.* **2014**, *276*, 1−33.
(12) Sessoli, R.; Powell, A. K. *Coord. Chem. Rev.* **2009**, *253*, 2328−2341.
(13) Bottrill, M.; Kwok, L.; Long, N. J. *Chem. Soc. Rev.* **2006**, *35*, 557−571.
(14) Layfield, R. A. *Organometallics* **2014**, *33*, 1084−1099.
(15) Ishikawa, N.; Sugita, M.; Ishikawa, T.; Koshihara, S.-y.; Kaizu, Y. *J. Am. Chem. Soc.* **2003**, *125*, 8694−8695.
(16) Ishikawa, N.; Sugita, M.; Ishikawa, T.; Koshihara, S.-y.; Kaizu, Y. *J. Phys. Chem. B* **2004**, *108*, 11265−11271.
(17) Jiang, S.-D.; Wang, B.-W.; Su, G.; Wang, Z.-M.; Gao, S. *Angew. Chem., Int. Ed.* **2010**, *49*, 7448−7451.
(18) Cucinotta, G.; Perfetti, M.; Luzon, J.; Etienne, M.; Car, P.-E.; Caneschi, A.; Calvez, G.; Bernot, K.; Sessoli, R. *Angew. Chem., Int. Ed.* **2012**, *51*, 1606−1610.
(19) Zhang, P.; Guo, Y.-N.; Tang, J. *Coord. Chem. Rev.* **2013**, *257*, 1728−1763.
(20) Luzon, J.; Sessoli, R. *Dalton Trans.* **2012**, *41*, 13556−13567.
(21) Anwar, M. U.; Thompson, L. K.; Dawe, L. N.; Habib, F.; Murugesu, M. *Chem. Commun.* **2012**, *48*, 4576−4578.
(22) Rinehart, J. D.; Long, J. R. *Chem. Sci.* **2011**, *2*, 2078−2085.
(23) Demir, S.; Zadrozny, J. M.; Nippe, M.; Long, J. R. *J. Am. Chem. Soc.* **2012**, *134*, 18546−18549.
(24) Bogani, L.; Wernsdorfer, W. *Nat. Mater.* **2008**, *7*, 179−186.
(25) Leuenberger, M. N.; Loss, D. *Nature* **2001**, *410*, 789−793.
(26) Yamanouchi, M.; Chiba, D.; Matsukura, F.; Ohno, H. *Nature* **2004**, *428*, 539−542.
(27) Saitoh, E.; Miyajima, H.; Yamaoka, T.; Tatara, G. *Nature* **2004**, *432*, 203−206.
(28) Gatteschi, D.; Caneschi, A.; Pardi, L.; Sessoli, R. *Science* **1994**, *265*, 1054−1058.
(29) Bagai, R.; Christou, G. *Chem. Soc. Rev.* **2009**, *38*, 1011−1026.
(30) Rocha, A. R.; Garcia-suarez, V. M.; Bailey, S. W.; Lambert, C. J.; Ferrer, J.; Sanvito, S. *Nat. Mater.* **2005**, *4*, 335−339.
(31) Rinehart, J. D.; Fang, M.; Evans, W. J.; Long, J. R. *Nat. Chem.* **2011**, *3*, 538−542.
(32) Vonci, M.; Boskovic, C. *Aust. J. Chem.* **2014**, *67*, 1542.
(33) Yamashita, A.; Watanabe, A.; Akine, S.; Nabeshima, T.; Nakano, M.; Yamamura, T.; Kajiwara, T. *Angew. Chem., Int. Ed.* **2011**, *50*, 4016−4019.
(34) Kajiwara, T.; Nakano, M.; Takahashi, K.; Takaishi, S.; Yamashita, M. *Chem. - Eur. J.* **2011**, *17*, 196−205.
(35) König, S. N.; Chilton, N. F.; Maichle-Mössmer, C.; Pineda, E. M.; Pugh, T.; Anwander, R.; Layfield, R. A. *Dalton Trans.* **2014**, *43*, 3035−3038.
(36) Das, S.; Hossain, S.; Dey, A.; Biswas, S.; Sutter, J.-P.; Chandrasekhar, V. *Inorg. Chem.* **2014**, *53*, 5020−5028.
(37) Gao, F.; Cui, L.; Liu, W.; Hu, L.; Zhong, Y.-W.; Li, Y.-Z.; Zuo, J.-L. *Inorg. Chem.* **2013**, *52*, 11164−11172.
(38) Fatila, E. M.; Rouzières, M.; Jennings, M. C.; Lough, A. J.; Clérac, R.; Preuss, K. E. *J. Am. Chem. Soc.* **2013**, *135*, 9596−9599.
(39) Thielemann, D. T.; Wagner, A. T.; Lan, Y.; Anson, C. E.; Gamer, M. T.; Powell, A. K.; Roesky, P. W. *Dalton Trans.* **2013**, *42*, 14794−14800.
(40) Anwar, M. U.; Dawe, L. N.; Tandon, S. S.; Bunge, S. D.; Thompson, L. K. *Dalton Trans.* **2013**, *42*, 7781−7794.
(41) Chandrasekhar, V.; Dey, A.; Das, S.; Rouzières, M.; Clérac, R. *Inorg. Chem.* **2013**, *52*, 2588−2598.
(42) Suzuki, K.; Sato, R.; Mizuno, N. *Chem. Sci.* **2013**, *4*, 596−600.
(43) Chandrasekhar, V.; Hossain, S.; Das, S.; Biswas, S.; Sutter, J.-P. *Inorg. Chem.* **2013**, *52*, 6346−6353.
(44) Le Roy, J. J.; Jeletic, M.; Gorelsky, S. I.; Korobkov, I.; Ungur, L.; Chibotaru, L. F.; Murugesu, M. *J. Am. Chem. Soc.* **2013**, *135*, 3502−3510.
(45) Sun, W.-B.; Han, B.-L.; Lin, P.-H.; Li, H.-F.; Chen, P.; Tian, Y.-M.; Murugesu, M.; Yan, P.-F. *Dalton Trans.* **2013**, *42*, 13397−13403.
(46) Wang, Y.-X.; Shi, W.; Li, H.; Song, Y.; Fang, L.; Lan, Y.; Powell, A. K.; Wernsdorfer, W.; Ungur, L.; Chibotaru, L. F.; Shen, M.; Cheng, P. *Chem. Sci.* **2012**, *3*, 3366−3370.
(47) Blagg, R. J.; Ungur, L.; Tuna, F.; Speak, J.; Comar, P.; Collison, D.; Wernsdorfer, W.; McInnes, E. J. L.; Chibotaru, L. F.; Winpenny, R. E. P. *Nat. Chem.* **2013**, *5*, 673−678.
(48) Chandrasekhar, V.; Das, S.; Dey, A.; Hossain, S.; Sutter, J.-P. *Inorg. Chem.* **2013**, *52*, 11956−11965.
(49) Tuna, F.; Smith, C. A.; Bodensteiner, M.; Ungur, L.; Chibotaru, L. F.; McInnes, E. J. L.; Winpenny, R. E. P.; Collison, D.; Layfield, R. A. *Angew. Chem., Int. Ed.* **2012**, *51*, 6976−6980.
(50) Völcker, F.; Lan, Y.; Powell, A. K.; ROesky, P. W. *Dalton Trans.* **2013**, *42*, 11471−11475.
(51) Chen, G.-J.; Gao, C.-Y.; Tian, J.-L.; Tang, J.; Gu, W.; Liu, X.; Yan, S.-P.; Liao, D.-Z.; Cheng, P. *Dalton Trans.* **2011**, *40*, 5579−5583.
(52) Blagg, R. J.; Muryn, C. A.; McInnes, E. J. L.; Tuna, F.; Winpenny, R. E. P. *Angew. Chem., Int. Ed.* **2011**, *50*, 6530−6533.
(53) Abbas, G.; Lan, Y.; Kostakis, G. E.; Wernsdorfer, W.; Anson, C. E.; Powell, A. K. *Inorg. Chem.* **2010**, *49*, 8067−8072.

DOI: 10.1021/acs.inorgchem.5b00899
Inorg. Chem. 2015, 54, 7846−7856

(54) AlDamen, M. A.; Cardona-Serra, S.; Clemente-Juan, J. M.; Coronado, E.; Gaita-Ariño, A.; Martí-Gastaldo, C.; Luis, F.; Montero, O. *Inorg. Chem.* **2009**, *48*, 3467−3479.
(55) Xue, S.; Zhao, L.; Guo, Y.-N.; Chen, X.-H.; Tang, J. *Chem. Commun.* **2012**, *48*, 7031−7033.
(56) Gamer, M. T.; Lan, Y.; Roesky, P. W.; Powell, A. K.; Clérac, R. *Inorg. Chem.* **2008**, *47*, 6581−6583.
(57) Lin, P.-H.; Burchell, T. J.; Ungur, L.; Chibotaru, L. F.; Wernsdorfer, W.; Murugesu, M. *Angew. Chem., Int. Ed.* **2009**, *48*, 9489−9492.
(58) Guo, Y.-N.; Xu, G.-F.; Gamez, P.; Zhao, L.; Lin, S.-Y.; Deng, R.; Tang, J.; Zhang, H.-J. *J. Am. Chem. Soc.* **2010**, *132*, 8538−8539.
(59) Bhunia, A.; Gamer, M. T.; Ungur, L.; Chibotaru, L. F.; Powell, A. K.; Lan, Y.; Roesky, P. W.; Menges, F.; Riehn, C.; Niedner-Schatteburg, G. *Inorg. Chem.* **2012**, *51*, 9589−9597.
(60) Shen, S.; Xue, S.; Lin, S.-Y.; Zhao, L.; Tang, J. *Dalton Trans.* **2013**, *42*, 10413−10416.
(61) Lin, S.-Y.; Zhao, L.; Guo, Y.-N.; Zhang, P.; Guo, Y.; Tang, J. *Inorg. Chem.* **2012**, *51*, 10522−10528.
(62) Hewitt, I. J.; Tang, J.; Madhu, N. T.; Anson, C. E.; Lan, Y.; Luzon, J.; Etienne, M.; Sessoli, R.; Powell, A. K. *Angew. Chem., Int. Ed.* **2010**, *49*, 6352−6356.
(63) Luzon, J.; Bernot, K.; Hewitt, I. J.; Anson, C. E.; Powell, A. K.; Sessoli, R. *Phys. Rev. Lett.* **2008**, *100*, 247205.
(64) Tang, J.; Hewitt, I.; Madhu, N. T.; Chastanet, G.; Wernsdorfer, W.; Anson, C. E.; Benelli, C.; Sessoli, R.; Powell, A. K. *Angew. Chem., Int. Ed.* **2006**, *45*, 1729−1733.
(65) McLellan, R.; Palacios, M. A.; Beavers, C. M.; Teat, S. J.; Brechin, E. K.; Dalgarno, S. J. *Chem. Commun.* **2013**, *49*, 9552−9554.
(66) Hewitt, I. J.; Lan, Y.; Anson, C. E.; Luzon, J.; Sessoli, R.; Powell, A. K. *Chem. Commun.* **2009**, 6765−6767.
(67) Lin, S.-Y.; Zhao, L.; Ke, H.; Guo, Y.-N.; Tang, J.; Guo, Y.; Dou, J. *Dalton Trans.* **2012**, *41*, 3248−3252.
(68) Ke, H.; Xu, G.-F.; Guo, Y.-N.; Gamez, P.; Beavers, C. M.; Teat, S. J.; Tang, J. *Chem. Commun.* **2010**, *46*, 6057−6059.
(69) Abbas, G.; Kostakis, G. E.; Lan, Y.; Powell, A. K. *Polyhedron* **2012**, *41*, 1−6.
(70) Langley, S. K.; Chilton, N. F.; Gass, I. A.; Moubaraki, B.; Murray, K. S. *Dalton Trans.* **2011**, *40*, 12656−12659.
(71) Gass, I. A.; Moubaraki, B.; Langley, S. K.; Batten, S. R.; Murray, K. S. *Chem. Commun.* **2012**, *48*, 2089−2091.
(72) Tian, H.; Zhao, L.; Lin, H.; Tang, J.; Li, G. *Chem. - Eur. J.* **2013**, *19*, 13235−13241.
(73) Roesky, P. W.; Bhunia, A.; Lan, Y.; Powell, A. K.; Kureti, S. *Chem. Commun.* **2011**, *47*, 2035−2037.
(74) Yadav, M.; Mereacre, V.; Lebedkin, S.; Kappes, M. M.; Powell, A. K.; Roesky, P. W. *Inorg. Chem.* **2015**, *54*, 773−781.
(75) Andrews, P. C.; Beck, T.; Fraser, B. H.; Junk, P. C.; Massi, M.; Moubaraki, B.; Murray, K. S.; Silberstein, M. *Polyhedron* **2009**, *28*, 2123−2130.
(76) Andrews, P. C.; Deacon, G. B.; Frank, R.; Fraser, B. H.; Junk, P. C.; MacLellan, J. G.; Massi, M.; Moubaraki, B.; Murray, K. S.; Silberstein, M. *Eur. J. Inorg. Chem.* **2009**, *2009*, 744−751.
(77) Roesky, P. W.; Canseco-Melchor, G.; Zulys, A. *Chem. Commun.* **2004**, 738−739.
(78) Datta, S.; Baskar, V.; Li, H.; Roesky, P. W. *Eur. J. Inorg. Chem.* **2007**, 4216−4220.
(79) Baskar, V.; Roesky, P. W. *Z. Anorg. Allg. Chem.* **2005**, *631*, 2782−2785.
(80) Andrews, P. C.; Beck, T.; Forsyth, C. M.; Fraser, B. H.; Junk, P. C.; Massi, M.; Roesky, P. W. *Dalton Trans.* **2007**, 5651−5654.
(81) Thielemann, D. T.; Wagner, A. T.; Lan, Y.; Oña-Burgos, P.; Fernández, I.; Rösch, E. S.; Kölmel, D. K.; Powell, A. K.; Bräse, S.; Roesky, P. W. *Chem. - Eur. J.* **2015**, *21*, 2713−2713.
(82) Thielemann, D. T.; Wagner, A. T.; Rösch, E.; Kölmel, D. K.; Heck, J. G.; Rudat, B.; Neumaier, M.; Feldmann, C.; Schepers, U.; Bräse, S.; Roesky, P. W. *J. Am. Chem. Soc.* **2013**, *135*, 7454−7457.
(83) Sheldrick, G. M. *Acta Crystallogr., Sect. A: Found. Crystallogr.* **2008**, *64*, 112−122.
(84) Peng, J.-B.; Kong, X.-J.; Ren, Y.-P.; Long, L.-S.; Huang, R.-B.; Zheng, L.-S. *Inorg. Chem.* **2012**, *51*, 2186−2190.
(85) Goura, J.; Walsh, J. P. S.; Tuna, F.; Chandrasekhar, V. *Inorg. Chem.* **2014**, *53*, 3385−3391.
(86) Bi, Y.; Wang, X.-T.; Liao, W.; Wang, X.; Deng, R.; Zhang, H.; Gao, S. *Inorg. Chem.* **2009**, *48*, 11743−11747.
(87) Xue, S.; Zhao, L.; Guo, Y.-N.; Chen, X.-H.; Tang, J. *Chem. Commun.* **2012**, *48*, 7031−7033.

DOI: 10.1021/acs.inorgchem.5b00899
Inorg. Chem. 2015, 54, 7846−7856